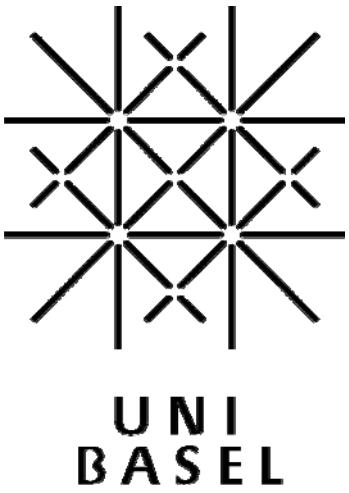

Organizing committee of SSD5:

The groups of:

Prof. Wolfgang Meier,

Prof. Thomas Pfohl,

PD. Dr. Cornelia Palivan.

Front page images: http://www.eng.cam.ac.uk/photocomp/2009/

Program

10:00	**Arrival**	
10:15 – 10:30	Opening Notes	
Session 1: Colloids and Polymers		
10:30 – 11:10	**Invited talk**: Special behaviors of responsive microgels in bulk and at interfaces	Prof. Dr. Walter Richtering RWTH Aachen University
11:10 – 11:30	Method for evaluating the Ostwald ripening kinetics of air microbubbles	J. C. Germain (Nestlé)
11:30 – 11:50	Photonic crystal and colloidal particle fabrication via 3D laser nanolithography	J. Haberko (Uni Fribourg)
11:50 – 12:10	Towards model bioactive polymer self-assembly	C. Vebert (Uni Geneva)
12:10 – 13:00	Lunch	
13:00 – 13:40	Poster session 1	
Session 2: Soft Matter and Biological systems		
13:40 – 14:00	pH-Responsive lyotropic liquid crystals for controlled drug delivery	R. Negrini (ETH)
14:00 – 14:20	Mechanobiology: correlation between mechanical stability of microcapsules studied by AFM and impact of cell-induced stresses	M. Delcea (Uni Basel)
14:20 – 14:40	Mechanical growth regulation of Drosophila wing imaginal discs	C. M. Aegerter (Uni Zürich)
14:40 – 15:00	Non-kinetic modelling of the mechanical unfolding of multimodular proteins: theory and experiments	F. Benedetti (EPFL)
15:00 – 15:40	Coffee Break – Poster session 2	
Session 3: Mixed Session Including Phenomena at Interfaces		
15:40 – 16:00	Parenteral nanomedicine: pharmaceutical requirements for in-vivo performance and safety	A.Fisch (Novartis)
16:00 – 16:20	Optical Trapping Microrheology in Cultured Human Cells	E. Bertseva (EPFL)

16:20 – 16:40	Towards a better understanding of eye lens transparency and cataract formation	C. Jud (Uni Fribourg)
16:40 – 17:00	Shear-driven solidification of dilute colloidal suspensions	E. Del Gado (ETH)
17:00 – 17:10	Closing remarks	
17 :15	**End of SSD 5 - After conference party- city beach or Kaserne (depending on the weather)**	

ORAL CONTRIBUTIONS

Method for evaluating the Ostwald ripening kinetics of air microbubbles

Juan C. Germain, Deniz Z. Gunes, Hans J. Limbach, Jin-Mi Jung, Eric Hughes

Nestlé Research Center, Department of Food Science and Technology, Vers-chez-les-Blanc, Lausanne 26, CH-1000, Switzerland

The stability of foams (and of aerated system in general) is affected by three basic mechanisms: gravitational drainage, Ostwald ripening (also called disproportionation), and coalescence. Ostwald ripening, in particular, refers to the changes in bubble sizes due to gas diffusion driven by local differences in Laplace pressure, or by gas diffusion to a head space. This process can be strongly influenced by the bulk and interfacial rheological properties of the system [1]. It is therefore interesting to be able to modulate Ostwald ripening by adjusting the system properties in order to increase the stability of aerated products. To study the Ostwald ripening process, we have developed an observation cell adapted from the literature. Our system allows following the shrinkage of multiple microbubbles (50-150 μm in diameter) simultaneously while they dissolve under controlled conditions (temperature and bulk gas concentration). Bubble size was controlled using microfluidic methods, and generated at lw frequency. The gas concentration was measured and equilibrated with the atmosphere before measurement. This works describes the application of this set-up to study and compare the Ostwald ripening of bubbles stabilized in various systems : pure ware, SDS 0.1%, native β-lactoglobulin 0.1% pH 2, β-lactoglobulin fibers 0.1% pH 2. The diffusion coefficient of water was measured using NMR methods, and gas diffusion coefficients corrected proportionally to the water values. Bubble shrinkage curves obtained as a result of the analysis accurately illustrate the differences between the systems investigated. As expected, bubbles in pure water and SDS solutions shrink a rate directly linked to the surface tension values, whereas, those stabilized by proteins shrink at rates influenced by surface properties of the protein films. Good agreement between experimental curves and theoretical values was also obtained when the data was fitted to a simplified model describing the physical phenomenon.

[1] Kloek, W., Van Vliet, T. and Meinders M. (2001). Effect of bulk and interfacial rheological properties on bubble dissolution. J. Colloid Interf. Sci., 237:158–166.

Photonic crystal and colloidal particle fabrication via 3D laser nanolithography

Jakub Haberko

Department of Physics, University of Fribourg, Switzerland.
AGH University of Science and Technology, Cracow, Poland

INTRODUCTION: 3D laser nanolithography is a method that allows fabricating arbitrary 3D structures with a resolution well below 1 μm. In this technique ultrashort (≤100 fs) laser pulses are used to locally induce crosslinking in a polymer photoresist via a two-photon absorption process. As the probability of this process scales with light intensity squared, the crosslinking takes place only in the region of extremely high laser power in a small volume around the focal point, which is the source of high resolution.

RESULTS: In this talk I will present the possibility to fabricate photonic crystals of different design (e.g. woodpile structures or spiral photonic crystals) by means of this technique. In order to increase the refractive index contrast in the structure and hence the band-gap width, these structures may consecutively be coated or infiltrated with a high-index material with for instance the atomic layer deposition technique. Since within resolution limits one has full control of the shape and size of the structures, it is possible to adjust the position and depth of the photonic band-gap, which will also be shown in the talk. Furthermore, it is also possible to introduce random or structured defects into the structure, which allows introducing pass-bands within the band-gap. I will also present spiral colloidal particles fabricated with this technique with view of studying their interactions with liquid crystals.

.

TOWARDS MODEL BIOACTIVE POLYMER SELF-ASSEMBLY

D.Kedracki[1], L.Ploux[2], C.Vebert[1]

[1] *Department of Inorganic, Analytical and Applied Chemistry, University of Geneva, Switzerland.* [2] *Institut de Science des Matériaux de Mulhouse, CNRS, University of Haute-Alsace, Mulhouse, France.*

INTRODUCTION: Nowadays, there is a major interest in the design of bioactive polymeric materials. Some of the prominent examples are the developments of platforms for tissue engineering and the design of medical devices as well as carriers for drug or gene therapy. In this context, soft templates based on self-assembled nucleotide-based amphiphilic copolymers present a new class of very promising biologically active materials.

METHODS: Bioactive self-assemblies were prepared by the polymer modification of short nucleotide sequences with a hydrophobic poly(isobutylene) (PIB) segment through solid phase synthesis[1]. Self-assembly into vesicular structures in dilute aqueous solution enabled the design of nanoreactors. The permeability of the resulting nanocontainers was allowed by the functional incorporation of naturally occurring pore-forming proteins in the polymeric membrane. The self-assembled structures were further immobilized on surfaces via base pairing between the nucleotide sequences composing the self-assembled copolymers and the surface-tethered complementary sequences.

Using E.coli K12 wild and mutant strains, we observed the influence of the modified surfaces on the dynamic of bacterial attachment as well as on the number and the motility of adherent bacteria. Real-time observations were performed through confocal laser scanning microscopy. Image analysis was processed by using CellC and ImageJ softwares.

RESULTS: The bioactivity of the nanoreactors was assayed by the encapsulation of an enzyme. Enzymatic activity monitoring demonstrates the potential of this prodrug-drug system, which is functional and efficiently prevents the enzyme degradation in a non-favourable environment. We further demonstrated that surfaces coated with immobilized vesicular structures decrease the number of visible, adherent bacteria in comparison with surfaces presenting a similar surface chemistry (Figure 1).

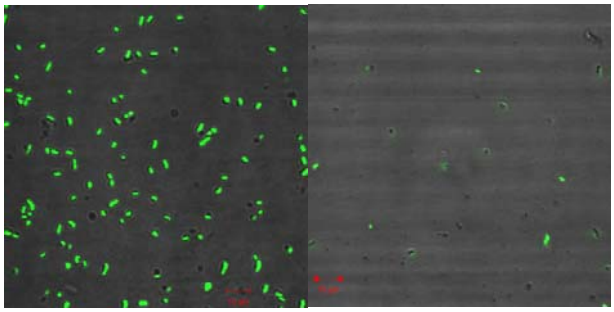

Fig. 1: Decreased number of visible, adherent bacteria on surfaces coated with immobilized vesicular structures in comparison with surfaces presenting a similar surface chemistry: bacterial response on surface tethered A_5G_7 linear nucleotide sequences (left) vs. vesicles self-assembled from poly(isobutylene)-modified nucleotide sequences immobilized on the surface modified with the T_5C_7 complementary sequence.

DISCUSSION & CONCLUSIONS: From the observations in dynamic conditions, we assume that the reduction of the number of adherent bacteria on surfaces coated with vesicular structures is due to an increased bacterial motility on the surface, leading to a high detachment rate. The bacterial motility is probably induced by the dissipative properties of the substrate, which does not offer anchoring points to the bacteria, therefore not allowing irreversible adhesion and further biofilm formation to occur. Aside from demonstrating the proof of concept of the preparation of bioactive surfaces based on surface-tethering of polymeric nanoreactors, this study provides novel and new evidences of the possibility to design anti-adhesive surfaces by exploiting the surface mechanical properties.

REFERENCES: [1] F. Teixeira *et al*. 2007 ; *Chem. Commun*. 11: 1130-1132.

ACKNOWLEDGEMENTS: Authors want to acknowledge the Swiss National Sceicne Foundation for Research (PPOOP2-128380), the NCCR-NANO and the "CRUS Stipend für Cotutelle de thèse, Programme 2010" for providing financial support to this project.

pH-Responsive Lyotropic Liquid Crystals for Controlled Drug Delivery

R. Negrini and R. Mezzenga

ETH Zürich, Food & Soft Materials Science, Zürich, Switzerland.

INTRODUCTION: Stimuli-responsive drug delivery systems can undergo suitable changes in response to specific environmental fluctuations or imposed variations of control parameters. Non-charged polar lipids are valuable candidates for this purpose due to their capacity to self-assemble in presence of water into a variety of reversed lyotropic liquid crystals (LLC) depending on different variables. They show thermodynamically stable aqueous channels organized either in a 3D bicontinuous structure in the cubic phases or in a 1D parallel way in the hexagonal phases while the lipid tails occupy the region in between the channels, which makes them suitable nano-carries for both hydrophilic and hydrophobic drugs [1]. In particular, the release of hydrophilic drugs from LLCs is a diffusion controlled process regulated by both the size of the aqueous channels and the symmetry of the mesophase [2], therefore it is a priori possible to trigger structural changes which are reflected directly on the release rate of the drugs.

METHODS: The LLCs were prepared by mixing the lipid blend (Dimodan and linoleic acid) and water solution at the required pH and loaded or not by phloroglucinol (model drug), depending on the specific experiment. In vitro drug release and diffusion experiments were performed in triplicate sets for the pHs studied using an home-built set-up. UV-Vis spectrometer was used to measure the concentration of the drug and the LC mesophase characterized by Cross Polarized Light Microscope (CPOM) and small angle X-ray diffraction (SAXS).

RESULTS: Qualitative analysis using CPOM show that at low pH, the transition temperature between bicontinuous cubic and reverse hexagonal phase decreases in the case of the Dimodan:linoleic acid LLCs compare to the Dimodan LLCs; the result are confirmed by SAXS which reveals the presence of the Im3m bicontinuous cubic phase at pH 7 and the H_{II} reverse hexagonal phase at pH 2. The Higuchi equation (1) [3]:

$$Q=2\ C0\ \sqrt{(D\ t/\pi)} \qquad (1)$$

allows direct comparison between the different release rates of the drug from the two different mesophases and, therefore, to conclude that the bicontinuous cubic phase (3D) releases four times faster than the reverse hexagonal phase (1D).

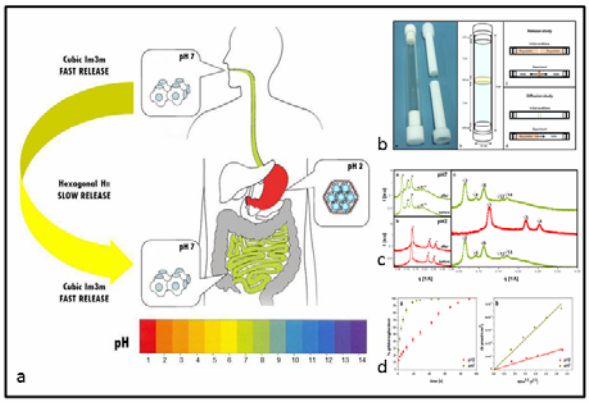

Fig. 1: a) Outline of the proposed pH-responsive drug delivery strategy across the gastrointestinal tract; b) Home-built set-up; c) SAXS curves at different pHs; d) Release profiles at different pHs (readapted from reference [4])

DISCUSSION & CONCLUSIONS: The system, composed by monolinolein and linoleic acid, in presence of excess water at 37°C and 150mM ionic strength, is specifically designed to reversibly change from a reverse Im3m bicontinuous cubic phase to a H_{II} reverse columnar hexagonal phase, when changing the pH from neutral to acidic conditions. The pH-responsiveness is provided by the linoleic acid, which being a weak acid (pKa≈5), is in the de-protonated charged state at pH 7 and mainly neutral at pH 2, imposing changes in the critical packing parameter (CPP) of the LLC. Due to the 3D organization of the water channels in the cubic phase, in contrast to the 1D organization in the reverse hexagonal phase, diffusion of the drug at pH 7 occurs four times faster than at pH 2. The resulting pH-responsive food-grade nano-carrier can be efficiently used to spontaneously trigger the release of drugs in the gastrointestinal tract (pH 7), while preventing premature release in the stomach environment (pH<2).

REFERENCES: [1] J. C Shah; **2001**; *M. Adv. Drug Delivery Rev.*; 47:229-250. [2] J. Clogston; **2005**; *Control. Rel.*; 107:97-111. [3] W.I. Higuchi; **1967**; *J. Pharm. Sci.*; 56:315-324. [4] R. Negrini; **xxxx**; *Langmuir*; xxx.

ACKNOWLEDGEMENTS: We acknowledge Dr. Sanchez Ferrer and H. Adelmann (ETHZ) for technical assistance and valuable discussions.

Mechanobiology: Correlation between Mechanical Stability of Microcapsules Studied by AFM and Impact of Cell-Induced Stresses

M.Delcea[1,2]

[1] *University of Basel, Basel, Switzerland.* [2] *Max-Planck Institute of Colloids and Interfaces, Potsdam, Germany.*

INTRODUCTION: Intracellular delivery of proteins, peptides, and other biomolecules by microcapsules is of growing importance not only in applied biomedical research, but also in fundamental cell biology [1]. Although microcapsules have the potential to reveal information about mechanobiology and cell mechanics, previous investigations of their mechanical properties have only been used for designing delivery vehicles with improved mechanical strength [2-4].
A correlation between mechanical and release properties of microcapsules studied in the context of intracellular incorporation has been established.

METHODS: In a novel approach, the forces inducing the release of encapsulated material from polymeric microcapsules are evaluated in an ex situ experiment using a combination of colloidal probe AFM with a fluorescence microscope (see Figure 1).

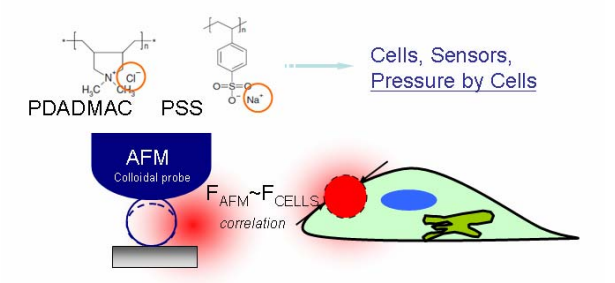

Figure 1. Schematics representing the use of capsules made of synthetic polymers as sensors to estimate the force exerted by cells upon intracellular incorporation.

To accomplish such goals, microcapsules with different mechanical properties were prepared, critical rupture forces were characterized in an ex-situ experiment using colloidal probe AFM, and these results were compared with cell studies. The capsule carriers used in this work exhibit a well-defined morphology, adjusted by thermal treatment that allows shrinking of the capsules in a controlled manner.

RESULTS:
The properties of microcapsules shrunk at 55° C (Figure 2a) 60° C (Figure 2b) and 70° C (Figure 2c) were investigated. Forces and deformation of microcapsules are measured by the colloidal probe technique [5]. It can be seen from Figure 2d that microcapsules shrunk at 70° C are the stiffest. Even when applying loads of 4 µN the deformation does not exceed 8% for such microcapsules.

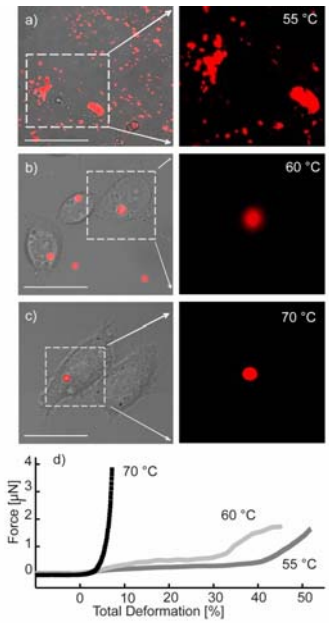

Figure 2. Images (differential interference contrast and red fluorescence channels are superimposed) of live Vero (African green monkey kidney) cells after intracellular incorporation of filled polymeric microcapsules shrunk at a) 55 ° C, b) 60 ° C, and c) 70 ° C. d) Force versus deformation curves for microcapsules shrunk at 55 ° C (grey line), 60 ° C (light grey line), and 70 ° C (black line). The scale bars correspond to 15 µ m.

REFERENCES: [1] R. Palankar et al.; **2009**; *Small* 5: 2168.
[2] R. Müller et al.; **2005**; *Macromolecules* 38: 9766.
[3] A. Fery and R. Weinkamer , **2007;** *Polymer* 48*:* 7221.
[4] B. S. Kim et al.; **2005**; *Macromulecules* 38: 5214.
[5] P. A. L. Fernandes et al.; **2010**; *Soft Matter* 6: 1879.

Mechanical growth regulation of Drosophila wing imaginal discs

C.M. Aegerter[1], U.Nienhaus[1], T.Schluck[1], M.B. Heimlicher[2], K. Basler[2], and T. Aegerter-Wilmsen[2]

[1] Physik-Institut [2] Institute of molecular life sciences

University of Zürich,Winterthurerstr. 190, 8057 Zürich, Switzerland.

INTRODUCTION: Mechanical growth regulation has been implicated to provide an avenue to explain several conundrums in the growth of the wing of the fruit fly Drosophila melanogaster[1,2]. Among these are the determination of final size of the wing as well as uniform growth in the presence of graded growth factors[3]. Here, we will present experimental as well as theoretical approaches to support the notion of mechanical growth regulation in the wing imaginal disc of Drosophila.

For the study of growth regulation of the fly wing, the precursor organ in the fly larva, the wing imaginal disc is studied. This is because almost all growth takes place in the larval stages and the final wing is formed through rearrangement of the tissue during metamorphosis[4]. Using a simple theoretical model of the growth of a wing imaginal disc, we have shown that it is possible to explain wing disc growth via the presence of mechanical feedback[2]. However, the direct demonstration of mechanical growth regulation has proven difficult due to the lack of appropriate in-vitro culturing systems for these tissues.

RESULTS: There is however indirect evidence for the mechanical growth regulation. This comes from three sources. Firstly, a direct investigation of the cell shape distribution within the wing disc shows that there are inhomogeneous stresses in this tissue, as evidenced by the present strains[5]. Second, photoelasticity measurements likewise show these graded stresses within the tissue[6,7]. Thus there is evidence that inhomogeneous stresses, which are necessary for the mechanical growth regulation are indeed present. Thirdly, we study the topology of the tissue, which is determined by the different division rates of the cells (see Figure 1). Depending on the cell cycle time, a cell obtains a different number of neighbours, thus determining the distribution of neighbour numbers. We have studied this both for mitotic cells and non-dividing cells[8]. Together with model simulations of the process, this allows a study of the influence of cell strain on the division rate of such a cell. These results indicate that there is a direct dependence of growth rate on cell strain, thus providing further evidence for mechanical growth regulation of the wing imaginal disc.

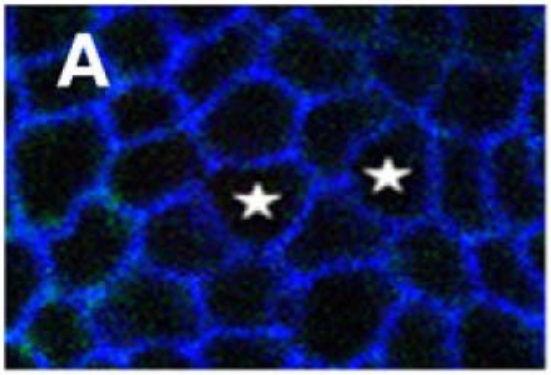

Fig. 1: Cell shapes in the wing imaginal disc, imaged using fluorescently labelled cell junction proteins.

DISCUSSION & CONCLUSIONS: Through three different ways, we provide indirect evidence for mechanical growth regulation in the wing imaginal disc of Drosophila. This encompasses both the presence of inhomogeneous stresses due to growth as well as the dependence of the growth rates on these inhomogeneous stresses.

REFERENCES: [1] L. Hufnagel *et al.* Proc. Nat. Acad. Sci (USA) *104*, 3835 **2007**.

[2] T. Aegerter-Wilmsen, C.M. Aegerter, E. Hafen, and K. Basler, Mech. Dev. *124*, 318 **2007.**

[3] M. Milan*, S: Campuzano and A. Garcia-Bellido* Proc. Nat. Acad. Sci (USA) *93*, 640 **1996**

[4] L. Wolpert *et al.*, *Principles of Development*, Oxford Univ. Press **2005**.

[5] M. B. Heimlicher, Master thesis University of Zurich **2011**.

[6] U. Nienhaus, T Aegerter-Wilmsen and C.M. Aegerter, Mech. Dev. *126*, 942 **2009.**

[7] T. Schluck and C.M. Aegerter, Europ. Phys. J. E *33*, 111 **2010.**

[8] T. Aegerter-Wilmsen *et al.* Development *137*, 499 **2010.**

ACKNOWLEDGEMENTS: This work was supported by the Swiss National Science Foundation and SystemsX.ch in the framework of the WingX RTD.

Non-kinetic modelling of the mechanical unfolding of multimodular proteins: theory and experiments

F. Benedetti[1], C. Micheletti[2], G. Bussi[2,3] S. Sekatskii[1] and G. Dietler[1]

[1] *EPF Lausanne, Lausanne, Switzerland.*

[2] *Sissa, Trieste, Italy.*

[3] *CNR-IOM Democritos and SISSA unit of the Italian Institute of Technology.*

INTRODUCTION: We introduce and discuss a novel approach for analyzing force spectroscopy experiments on multimodular proteins[1-2]. The relationship between the histograms of the unfolding forces for different peaks, corresponding to a different number of not-yet-unfolded protein modules, is highlighted. The relationship is such that the sole distribution of the forces for one unfolding peak can be used to predict the unfolding forces for other peaks. The prediction accuracy is so high that the predicted average unfolding forces corresponding to each peak for the GB1 construct are within only 5pN of the averaged directly-measured values. Experimental data are also used to illustrate how the limitations of standard kinetic models can be aptly circumvented by the proposed approach.

METHODS: GB1 polyproteins pulled with an atomic force microscope, Monte Carlo and Langevin dynamic simulations have been used to produce Force Spectroscopy curves. All of these methods give curves similar to Fig. 1.

RESULTS: 47 experimental force curves from $(GB1)_8$, 350 Langevin curves and one thousand MC force curves have been analyzed. The results of our prediction method, that we called "Back Calculation" (BC), based on the statistics of the peaks in position "1" for the $(GB1)_8$ experiment is reported in Fig.2. Moreover an analytical approach has been developed, based on this we have been also able to explain the behaviour of the standard deviation as the function of the peak order.

DISCUSSION & CONCLUSIONS: The BC method introduced here has some advantages in respect to others prediction methods. First it does not need the estimation of the kinetic parameters. Second, its implementation is straightforward and relies only on the estimation of the cumulative function of one of the peaks in a chain of "n" modules. The analytical method instead allow a good prediction of the peak force and, for our knowledge, it is the first time that the behaviour of the standard deviation for each peak has been explained.

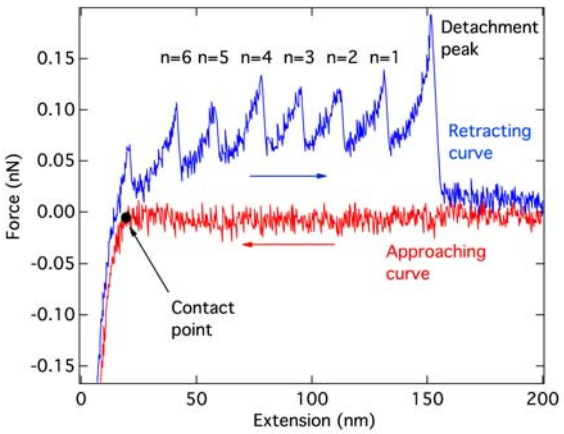

Fig. 1: A typical force curve obtained during the extension of $(GB1)_8$ using an atomic force microscope. The position of the peaks and the special regions of the graph are highlighted.

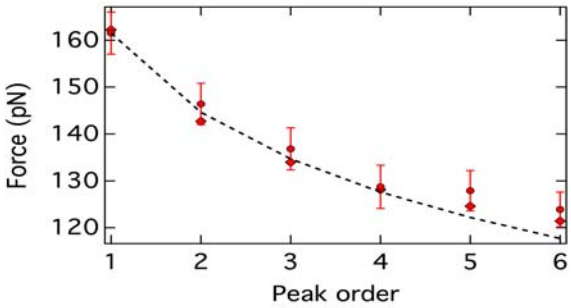

Fig. 2: Average unfolding force vs peak order for the experimental data on GB1 (red circles), BC (red diamonds), the dotted line is instead the non-kinetic model developed starting from Bell-Evans theory.

REFERENCES:

[1] Y. Cao and H. Li. 2007. Nature Materials 6:109–114.

[2] F. Benedetti, S. K. Sekatskii, and G. Dietler. 2011. Journal of Scanning Probe Microscopy 6:1–6.

ACKNOWLEDGEMENTS: Swiss National Science Foundation (grant no. 205320-131828) and Italian Ministry of Education are grateful acknowledged.

Parenteral Nanomedicine: Pharmaceutical requirements for in-vivo performance and safety

Andreas Fisch

Fellow, Novartis Pharma AG, Basel

Market sucess of Nanomedicine products has proven its clinical benefit and value. Nanosuspensions, liposomes or nanosized drug conjugate formulations may enable the parenteral delivery of poorly soluble drugs. In addition, nanoparticulate formulations may lead to a targeting effect that enables higher drug efficacy at a lower adverse effect rate compared to a simple parenteral solution formulation.

Therefore, Nanotechnology is considered as one of the key technologies of the 21st century stimulating intensive interdisciplinary research and development activities in different scientific areas of Academia and in the Pharmaceutical industry as well as intense collaboration of both communities.

However, the development of such Nanomedicine products also involves a higher level of complexity and risk. Thus the innovation stakeholders from Academia have to be aware of the requirements of the Pharmaceutical Industry and the regulatory environment to anticipate the critical aspects for parenteral Nanomedicine at an already stage of development. This includes formulation requirments, processability and scalability as well as biocompatibility aspects.

Nanomedicine must be well characterized, the physicochemical and chemical stability must be assured both in vitro and in vivo and the release kinetics needs to be well controlled. Excipients should be excretable and safe. The technology should be flexible for delivery of molecules with a wide range of physicochemical properties and doses: simplicity of composition and manufacturing beats complexity. Manufacturing under cGMP and viable regulatory acceptance is key.

On the other hand, biocompatibility of parenteral Nanomedicine is of fundamental importance to minimize undesired adverse reaction upon administration. Acceptably low levels of hemolysis, thrombogenicity, complement activation and accelerated blood clearance of the Nanomedicine has to be assured by the choice of excipients, composition and particle size. Adequate biocompatibility test systems should be established in the early development and used for formulation screening.

The speed and extent of utilization of the great opportunities of the highly innovative field of Nanomedicine in industrial drug product development depends heavily on the shared understanding and collaboration of innovation stakeholders in Basic research and Pharmaceutical industry.

Optical Trapping Microrheology in Cultured Human Cells

E.Bertseva[1], D.Grebenkov[2], S.Jeney[1], L.Forro[1]

[1] Laboratory of Physics of Complex Matter, Ecole polytechnique federale de Lausanne (EPFL), Station 3, CH–1015 Lausanne VD, Switzerland. [2] Laboratoire de Physique de la Matière Condensée, CNRS – Ecole Polytechnique, F-91128 Palaiseau, France.

INTRODUCTION: We present the microrheological study of the two close human epithelial cell lines: non-malignant HCV29 and cancerous T24. The optical tweezers tracking was applied to extract the trajectories of endogenous lipid granules which were analyzed using a recently proposed equation for mean square displacement (MSD)[1].

METHODS: The set-up is based on a Nd:YAG laser, with the wavelength of 1064 nm. The endogenous granules of diameter about 0.4 μm have been chosen as the microrheological tracers, and the tracer trajectory is recorded through the back focal plane interferometric position detection.

RESULTS: Our 1MHz detection scheme has allowed to observe the subdiffusion inside the living cells for the lag times region 10^{-5}-10^{-3} s. At long time the MSD becomes influenced by the optical potential and tends to a constant. Recently, Desposito and Vinales have derived the analytical formula for the MSD in the case of subdiffusion influenced by an optical trap[1]:

$$\left\langle \Delta r^2(t) \right\rangle = \frac{2k_B T}{k} n\left(1 - E_\alpha\left(-\frac{k}{\gamma_\alpha} t^\alpha\right)\right), \qquad (1)$$

Where k is the trap spring constant, α is the subdiffusion exponent and E_α is the Mittag-Leffler function. The parameters obtained by fitting this equation to the experimental MSDs are summarized in Table 1.

Table 1. Parameters obtained from fitting Eq. (1) to the MSD of the granules inside cells. The uncertainty is the standard deviation of parameters between different granules.

	Cell line	$2k_BT/k$ (nm^2)	α	$X_3 = \left(\frac{k}{\gamma_\alpha}\right)^{\frac{1}{\alpha}}$ (Hz)
k_1	HCV29	1277±721	0.70±0.07	11±9
k_1	T24	1413±669	0.69±0.07	6±3
k_2	HCV29	679±258	0.73±0.02	36±18
k_2	T24	487±198	0.67±0.05	10±7
k_3	HCV29	186±58	0.73±0.04	172±88
k_3	T24	218±52	0.75±0.03	166±103

DISCUSSION & CONCLUSIONS:

At high frequencies we have not found any difference between the two cell types, contrarily to the previous results obtained by AFM[2]. For both cell lines the subdiffusion exponent, α was found close to ¾, the value predicted by the theory of semiflexible polymers. But the crossover frequency X_3, was found smaller for the cancerous cells for all datasets. It corresponds to passage to the confined regime at longer times. We attribute it to the bigger impact of molecular motors. The cancerous cells present the larger MSD at long lag time confirms the literature results for other cell lines[3] and provides the explanation for the AFM results which have been obtained at low frequency.

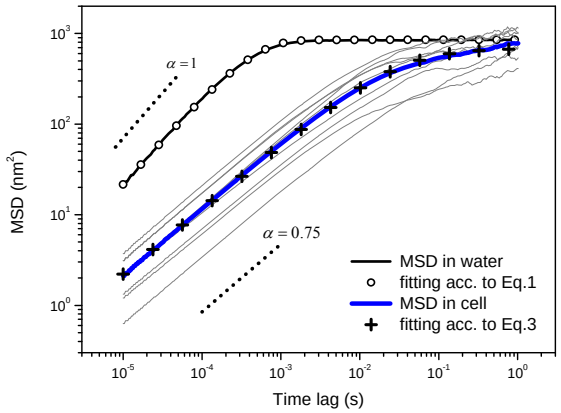

Figure 1. The mean square displacement (MSD) of the 0.4 μm diameter tracer in the purely viscous medium outside the cell (black line) and inside the HCV cell (blue line) where it presents the subdiffusive scaling. Thin grey lines show the MSDs of different granules inside the cells.

REFERENCES: [1] M. A. Desposito and A. D. Vinales; **2009**; *Physical Review E*; 80: 021111-021117. [2] S. E. Cross and et al; **2008**; *Nanotechnology*; 19: 384003. [3] Y. Li, J. Schnekenburger and M. H. G. Duits, *Journal of Biomedical Optics*, 2009, **14**, 064005

ACKNOWLEDGEMENTS: The authors thank Dr. M. Lekka for providing the cell lines, and Dr. J.Lekki for the technical support in the instrumental part. We also thank Dr. A.Kulik for useful discussions. Elena Bertseva thanks for support the National Swiss Fond MHV subsidy PMPDP2_134178/1.

Towards a better understanding of eye lens transparency and cataract formation

C. Jud[1], N. Mahmoudi[1], Y. Umehara[1], A. Stradner[2], P. Schurtenberger[2]

[1]*Adolphe Merkle Institute, University of Fribourg, Switzerland.*
[2]*Physical Chemistry, Lund University, Sweden.*

INTRODUCTION: For proper vision, an impeccably transparent eye lens is indispensable. This is achieved by a complex architecture and a unique protein composition. Any disturbance of this highly ordered system leads to clouding of the lens. This so called cataract is very frequent in old people and the leading cause for blindness. Understanding interparticle interactions in eye lens proteins is of central importance because of their biological and medical relevance for cataract formation. In addition, due to their easily tunable interaction potentials, the eye lens proteins of the gamma-crystallin group are particularly interesting and ideally suited as well-defined model systems for colloids.

METHODS: In the present study we investigated the structural and dynamic properties of gammaB protein solutions up to concentrations corresponding to those found in the eye lens. By combining small-angle X-ray scattering (SAXS) with light scattering we analysed the behaviour of gammaB in two different phosphate buffers. One buffer contained light water only whereas the other was a mixture of 50 % light, 50 % heavy water.

RESULTS: The use of heavy water allowed us to increase the temperature of the critical point by about 8°C. From SAXS data, we have obtained gammaB structure factors versus concentration (ranging from 34 mg/mL to 432 mg/mL) and temperature (0-35°C).

Shear-driven solidification of dilute colloidal suspensions

A. Zaccone[1], D. Gentili[1], H. Wu[1], M. Morbidelli[1] and E. Del Gado[2]

[1] *Department of Chemistry and Applied Biosciences, ETH Zürich*
[2] *Department of Civil, Environmental and Geomatic Engineering, ETH Zürich*

Shear-driven solidification of diluted colloidal suspensions has dramatic impact on their applications, ranging from industrial making of paints to artificial or natural microfluidic devices and is a prototype of far from equilibrium transitions. We rationalize a set of experiments on dilute, charge-stabilized colloidal suspensions, and show that shear-induced solidification is the consequence of the interplay between the shear-induced breakage and formation of large non-Brownian clusters. While their size remains constant due to breakage, their number density increases with the shearing-time. Upon flow cessation, the dense packing of clusters interconnects into a rigid state by means of *grainy* bonds, each involving a large number of primary colloidal bonds (1,2). The emerging picture of shear-driven solidification in dilute colloidal suspensions combines colloidal gelation in Brownian suspensions and jamming in athermal systems.

(1) A. Zaccone, D. Gentili, H. Wu, M. Morbidelli and E. Del Gado, Phys. Rev. Lett. **106**, 138301 (2011)
(2) A. Zaccone, H. Wu and E. Del Gado, Phys. Rev. Lett. **103**, 208301 (2009)

POSTER CONTRIBUTIONS

Solid-supported biomimetic block copolymer membranes

S.Toughraï, E. Rakhmatullina, V. Malinova, WP.Meier[1]

[1] *Department of Chemistry, University of Basel, Klingelbergstrasse 80, CH-4056 Basel, Switzerland.*

INTRODUCTION: The functionalization of surfaces through biomimetic block copolymer membranes aims at developing smart surfaces for biotechnological applications such as biosensing. Amphiphilic block copolymer membranes were chosen instead of lipid membranes as mimics of biological membranes because of their properties, such as thickness, chemical and mechanical stability, lower permeability, fluidity, mobility, etc. Upon insertion of membrane proteins, these systems could allow for the preparation of mechanically and chemically robust and air-stable biosensor devices.

METHODS: Surface-initiated atom transfer radical polymerization (ATRP) provides a good control of the brush thickness by controlling polymer molecular weight and by initiating polymerization of a second monomer from the chain end of the first. Poly(2-hydroxyethyl methacrylate)-b-poly(n-butyl methacrylate)-b-poly(2-hydroxyethyl methacrylate), PHEMA-b-PBMA-b-PHEMA block copolymers were synthesized with the first PHEMA block anchored to a self-assembled monolayer on the gold surface while the other PHEMA block exposed to the outer surface. To this end, a self-assembled monolayer of ($BrC\text{-}(CH_3)_2COO(CH_2)_{11}S)_2$) initiator was formed through a covalent binding of disulfides to gold. Then, HEMA monomer was polymerized by ATRP. The first PHEMA block initiated the polymerization of BMA. Subsequently, the second PBMA block again initiated HEMA polymerization, thus resulting in a triblock copolymer membrane anchored to the gold substrate. Block copolymer brushes were prepared with different block lengths and characterized both on the gold surfaces and − after detaching from the solid support, − in solution.

RESULTS[1]: To test the solvent response behaviour of the triblock copolymer, block-selective solvent as well as a good common solvent for the triblock system were used for swelling experiments. Ethanol was chosen as a good solvent for the triblock copolymer chains, whereas hexane and water selectively swell the PBMA and PHEMA blocks, respectively. The PHEMA blocks swell considerably in water, whereas the hydrophobic PBMA block tends to avoid contacting the aqueous surrounding. However, the phase segregation was reversible because the reimmersion of the sample into one of three tested solvents resulted in reproducible morphologies. Figure 1(a) shows the 3D topography image of the wet copolymer chains on the gold surface. After drying, the sample acquired a nanodomain topography of the surface [Fig. 1(b)].

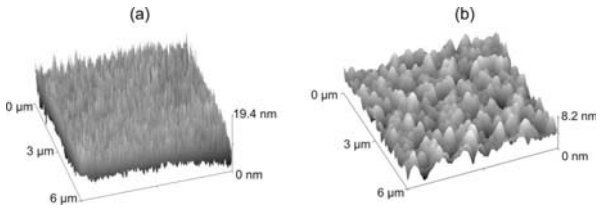

Fig. 1: Contact mode AFM analysis of the amphiphilic triblock copolymer membrane in water (a) and after sample drying (b).

DISCUSSION & CONCLUSIONS: Upon swelling in water, the brush-like structure of the macromolecules conforms to a stretched conformation of the PHEMA chains. Drying most probably causes a collapse of the polymer brushes and thus formation of nanodomains. The reversibility of the phase segregation proves the covalent attachment of the block copolymer layer and shows the potential use of these block copolymer membranes as responsive surfaces. The amphiphilic character of the triblock copolymer brushes provided a responsive surface that showed a solvent dependent arrangement of the block copolymer chains, which was also reflected in the morphologies of the dried films. The polymer brushes with a hydrophilic-hydrophobic-hydrophilic sequence can be regarded as the first example of solid supported, biomimetic block copolymer membranes prepared by a "grafting-from" approach.

REFERENCES: [1] E. Rakhmatullina, et al. (2009) *J. Polym. Sci. A* **47**:1-13.

ACKNOWLEDGEMENTS: The authors thank Serena Belegrinou, Dr. Nico Bruns and Dr. Raffaello Masciadri for helpful discussions on the synthesis and characterization of the triblock copolymer brushes. This work is supported by the Swiss National Science Foundation.

Fluorescent Proteins as Mechanophores in Damage Self-reporting Fiber-reinforced Plastics

Ch. Müller, S. Löcher, T. Winkler, N. Bruns

University of Basel, Basel, Switzerland.

INTRODUCTION: Living organisms have developed ways to detect and report damage of their tissue. This is usually accomplished by nerve signals, e.g., in the form of pain, or by optical signals, e.g., by the dark red color of a bleeding wound. The indication of damaged tissue is crucial for an organism in order to start to protect the respective body part. In technical applications, polymer-based materials are often used as load-bearing materials because they are lightweight, possess excellent mechanical properties and are easy to manufacture into any desired shape. Fiber-reinforced plastics (FRP) in particular find application in the aerospace, the automotive and the sporting goods sector. However, FRPs do not visualize damage to alert the user of impeding danger. In order to avoid accidents, man-made polymeric materials that detect and report small scale structural damage before catastrophic failure occurs are highly desirable.

METHODS: Fiber-reinforced plastics consist of two main compounds: the fibers e.g. glass or carbon fibers and the matrix e.g. an epoxy resin. FRP are fragile to mechanical impact. Low velocity impacts can cause barely visible damage, e.g. delamination between the fibers and the matrix.
Fluorescent proteins are expected to lose fluorescence upon mechanical unfolding. We use enhanced yellow fluorescent protein (eYFP) as mechanophore, i.e. as a molecule that changes its color or its fluorescence properties upon application of mechanic stress or strain. The fibers were modified with these proteins and embedded into an epoxy resin.

We propose the following concept:

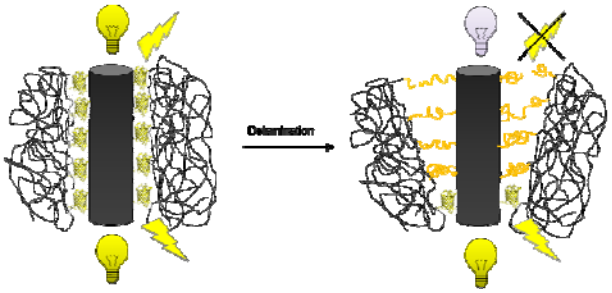

Delamination and micro cracks defects due to impact are reported by the proteins in the materials through vanishing of fluorescence. These signals can be observed by fluorescence microscopy.

RESULTS:

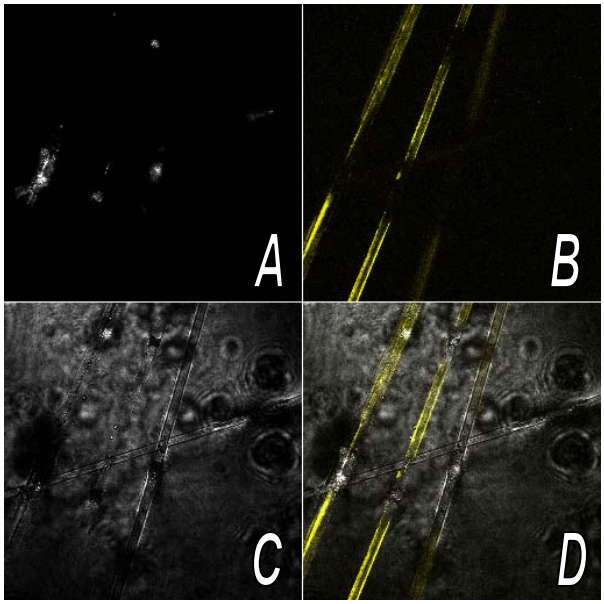

Fig. 1: Fluorescence microscope pictures of modified glass-fibers in epoxy resin after an impact. A) reflected light B) fluorescence light C) transmitted light D) overlay The micrographs have a dimensions of 230 x 230 µm. The glass-fibers have a thickness of 9 µm.

DISCUSSION & CONCLUSIONS: The concept proposed was proven to be working with glass-fibers (Fig. 1) and carbon-fibers embedded in a commercial, two component epoxy resin. The fluorescence intensity and the mechanophore response were shown to depend on the surface properties and on the immobilization protocol.

REFERENCES:

[1]S. Lörcher, N. Bruns, *patent application* GB 1009280.7, **2010**.
[2]S. Lörcher, T. Winkler, Ch. Müller, M. G. Nussbaumer, N. Bruns, *manuscript in preparation*, **2011**.

ACKNOWLEDGEMENTS: This work was funded by the Forschungsfonds der Universität Basel.

General Self-Assembly Mechanism Converting Hydrolyzed Globular Proteins Into Giant Multistranded Amyloid Ribbons

C. Lara, J. Adamcik, S. Jordens, R. Mezzenga

ETH Zürich, Zürich, Switzerland.

INTRODUCTION: Most proteins can form supramolecular fibrillar aggregates in vivo or in vitro, leading to neuronal and systemic pathologies and suggesting a common tendency of polypeptides to form amyloids. A general mechanism, covering all the steps from protein unfolding to fibrillation, is however still missing. Hen egg white lysozyme (HEWL) and β-lactoglobulin are both globular proteins forming amyloid fibrils in vitro but they differ in their molecular weights, primary to quaternary structures and physical properties, hindering any direct comparison in their amyloidosis pathway. In the present work, however, we intend to draw general conclusions on their fibrillation process, carried out under identical conditions, showing a cross-sectional growth in both multistranded protein systems, progressing up to unprecedented levels [1].

METHODS: Solutions of 2% w/w dialyzed protein were prepared in Milli-Q water at pH2 and incubated at 90 °C for 100 h. Formation of amyloid aggregates was detected as enhancement of the ThT fluorescence intensity with a Hitachi F-7000 fluorescence spectrophotometer. Tapping mode AFM was carried out on a Nanoscope VIII Multimode Scanning Force Microscope. Cryo-TEM samples (frozen hydrated fibers) were recorded at 100 kV. Electron micrographs were recorded using a Gatan 794 CCD camera. SDS-PAGE was run on Criterion precast gels 18% Tris-HCl at 100 V. Far-UV CD spectra of HEWL were recorded using a Jasco J-815 spectropolarimeter.

RESULTS: The number of filaments (each 10 nm wide and 4 nm high) per aggregate increases with incubation time and goes up to 17 filaments per fibril for HEWL (173 nm wide) and 16 filaments for β-lactoglobulin (160 nm). For both proteins, the formation of such similar large multistranded twisted and helical ribbons is concomitant with the hydrolysis of the pristine protein into very short fragments (< 6 kDa, SDS-PAGE) and is associated with further structural changes (CD). These results demonstrate that a complete hydrolysis of the protein at long incubation time leads to the newly reported massive ribbons.

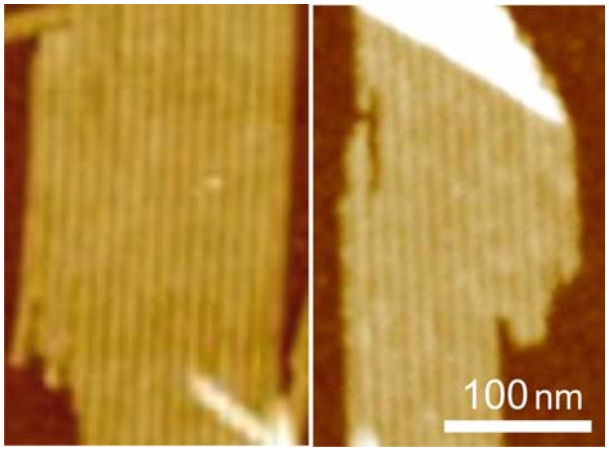

Fig. 1: AFM height images of the large amyloid ribbons of HEWL (left) and β-lactoglobulin (right).

DISCUSSION & CONCLUSIONS: These results open new perspectives in the understanding of fibrillation processes in globular proteins and amyloids polymorphism. AFM statistical analysis, SDS-PAGE and CD all provide convincing evidence that protein unfolding and complete hydrolysis are essential for the formation of large laminated aggregates and that small peptides fragments participate in the formation of these fibrils, irrespectively of the initial size of the protein. This could very well explain the observation that every fibril forming protein contains specific sequences responsible for fibrillation. The exceptional similarities in the fibrillation steps, building blocks and final amyloid structures for globular proteins as diverse as β-lactoglobulin and lysozyme and the direct analogies with aggregation processes in short synthetic polypeptides, further support a possible general common unfolding-fragmentation-aggregation mechanism for amyloidosis in globular proteins.

REFERENCES: [1] C. Lara, J. Adamcik, S. Jordens, R. Mezzenga; **2011**; *Biomacromolecules;* (in press) DOI**:** 10.1021/bm200216u.

ACKNOWLEDGEMENTS: We thank S. Handschin and F. Eichenseher for support with cryo-TEM imaging and SDS-PAGE experiments.

.

WHEN SOUND INTERFERES WITH HYDRODYNAMICS

Error! Hyperlink reference not valid.elushkin[1], **Error! Hyperlink reference not valid.** Winkler[2], **Error! Hyperlink reference not valid.** Foffi[1]

[1] *EPF Lausanne, Lausanne, Switzerland*
[2]*Forschungszentrum Juelich, Juelich, Germany.*

INTRODUCTION: It is well-known that the behaviour of small systems, e.g. of mesoscale objects in solution, is largely governed by the interplay of thermal fluctuations and hydrodynamics. This is because the typical relevant energy scales are of the order of one thermal energy k_BT. Another effect which can be crucially important for the dynamics of mesoscopic systems – the propagation of sound waves – is typically neglected, however. Frequently, neglecting sonic effects is reasonable, because the typical time scales are much shorter than the time scales of interest such as the hydrodynamic or the inertial time scales. However, in certain circumstances, neglecting the effects of sound can lead to serious errors in the description of the dynamical behaviour of a system. This is typically the case for very small, nanometre-scale solute objects in a solvent with a low velocity of sound. It has been predicted [1] that in this case, the interference of the propagation of a sound wave - caused by the motion of a colloidal particle in solution,- and the formation of the hydrodynamic vortex can lead to peculiar phenomena in the dynamics of the colloidal particle – namely, reversal of its velocity at times comparable to the sonic time scale.

METHODS: We perform computer simulations employing the method of multiparticle collision dynamics (MPC) [2,3] which is known to correctly capture both thermal fluctuations [4] and hydrodynamics [5] on coarse-grained length- and time-scales. Because the fluid in MPC obeys the equation of state of an ideal gas, the sound velocity is relatively small, i.e. the sonic time scale is relatively large and is typically of the same order of magnitude as the hydrodynamic and the ballistic time scales. Therefore, compressibility effects arise in MPC and make a significant contribution to the dynamics of the system in the simulation.

RESULTS: By performing computer simulations for various properties of the solvent and solute particles, we confirm the theoretical predictions of backtracking [1], i.e. velocity reversal of the solute particle at times corresponding to the sonic time scale. Furthermore, we explore the influence of backtracking on long-time observables, namely the long-time diffusion coefficient of the colloid.

REFERENCES:

[1] B. U. Felderhof, J. Chem. Phys. **123**, 044902 (2005).

[2] J. T. Padding, A. A. Louis, Phys. Rev. E **74**, 031402 (2006).

[3] G. Gompper, T. Ihle, D. M. Kroll, R. G. Winkler, Adv. Polym. Sci. **221**, 1 (2009).

[4] M. Belushkin, R. Livi, G. Foffi, Phys. Rev. Lett. (2011).

[5] T. Franosch, M. Grimm, M. Belushkin, F. Mor, G. Foffi, L. Forró, S. Jeney, submitted (2011).

[6] M. Belushkin, R. Winkler, G. Foffi, to be submitted (2011).

Tuning in-meso-Crystallized Lysozyme Polymorphism by Lyotropic Liquid Crystal Symmetry

Alexandru Zabara, Idit Amar-Yuli, Raffaele Mezzenga[1]

[1] *ETH Zurich, Food & Soft Materials Science, Institute of Food, Nutrition & Health, Zürich, Switzerland.*

Lipid-based lyotropic liquid crystals (LLCs) show great potential for applications in fields as diverse as food technology, cosmetics, pharmaceutics or structural biology. Recently, these systems have provided a viable alternative to the difficult process of membrane protein crystallization, owing to their similarities with cell membranes. Nonetheless, the process of *in-meso* crystallization of proteins still remains poorly understood.

In this study, we demonstrate that *in-meso* crystal morphologies of lsozyme (LSZ) -a model hydrophilic protein-, can be controlled by both the composition and symmetry of the mesophase, inferring a possible general influence of the LLC space group on the protein crystal polymorphism.

Lysozyme was crystallized *in-meso* from three common LLC phases (lamellar, inverse hexagonal and inverse bicontinuous cubic) composed of monolinolein and water. Different mixing ratios of mesophase to crystallization buffer were used in order to tune crystallization both in the bulk mesophase and in excess water conditions.

Two distinct mechanisms of crystallization were shown to take place depending on available water in the mesophases. In the bulk mesophases, protein nuclei form and grow within structural defects of the mesophase and partially dehydrate the system inducing order-to-order transitions of the liquid crystalline phase towards stable symmetries in conditions of lower hydration. The formed protein crystals eventually macrophase separate from the mesophase allowing the system to reach its final symmetry. On the other hand, when excess water is available, protein molecules diffuse from the water channels into the excess water, where the crystallization process can take place freely, and with little to no effect on the structure and symmetry of the lyotropic liquid crystals.

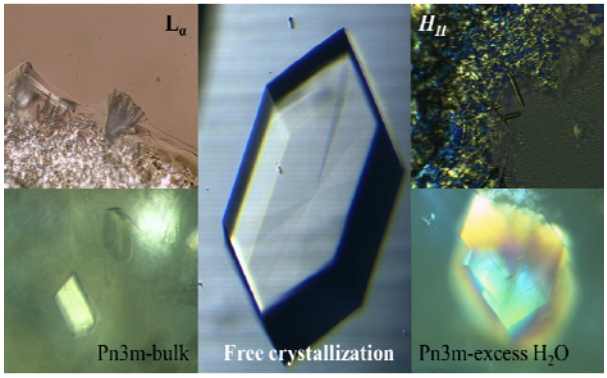

Fig. 1: Different polymorphic forms of lysozyme crystals obtained using the in-meso crystallization method from the different symmetries of the hosting mesophase.

At the same time it was clearly observed that the topology of the mesophase, the location of the mesophase in the phase diagram (bulk *vs.* excess water) and the inherent diffusion processes controlled by different mesophase symmetries all concur to determine the protein crystal space group and their macroscopic growth.

The present work brings further insights into the process of *in-meso* protein crystal formation and while it settles for the first time a general frame for engineering the protein crystals at the molecular and macroscopic level, it also highlights once more the subtle balance of the many parameters controlling this delicate, yet fascinating crystallization pathway.

A. Zabara, I. Amar.Yuli, R. Mezzenga, *Langmuir*, in press (2011).

Adsorption of Weak Polyelectrolytes on Charged Nanoparticles. Impact of Salt Valency, pH and Nanoparticle Charge Density. Monte Carlo Simulations.

F.Carnal[1], S.Stoll[1]

[1] *University of Geneva, F.-A. Forel Institute, Versoix, Switzerland.*

Complex formation between a weak flexible polyelectrolyte chain and one positively charged nanoparticle in presence of explicit counterions and salt particles is investigated using Monte Carlo simulations. The influence of parameters such as the nanoparticle surface charge density, salt valency, and solution property such as the pH on the chain protonation/deprotonation process and monomer adsorption at the nanoparticle surface are systematically investigated. It is shown that the nanoparticle presence significantly modifies chain acid/base and polyelectrolyte conformational properties. The importance of the attractive electrostatic interactions between the chain and the nanoparticle clearly promotes the chain deprotonation leading, at high pH and nanoparticle charge density, to fully wrapped polyelectrolyte at the nanoparticle surface. When the nanoparticle bare charge is overcompensated by the chain charges, counterions and salt particles condense at the surface of the polyelectrolyte-nanoparticle complex to compensate the excess of charges providing from the adsorbed polyelectrolyte chain. It is also shown that the complex formation is significantly affected by the salt valency. Indeed, with the presence of trivalent salt cations, a competition is observed between the nanoparticle and the trivalent cations. As a result, the amount of adsorbed monomers is less important than in the monovalent and divalent case and chain conformations are different due to the collapse of polyelectrolyte segments around trivalent cations out of the nanoparticle adsorption layer.

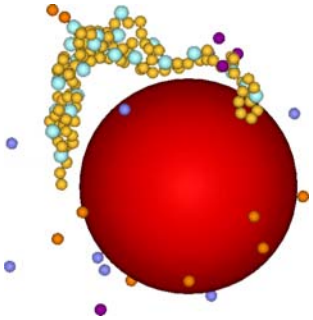

Fig. 1: Equilibrated conformation of a weak polyelectrolyte chain and one nanoparticle surrounded by trivalent salt.

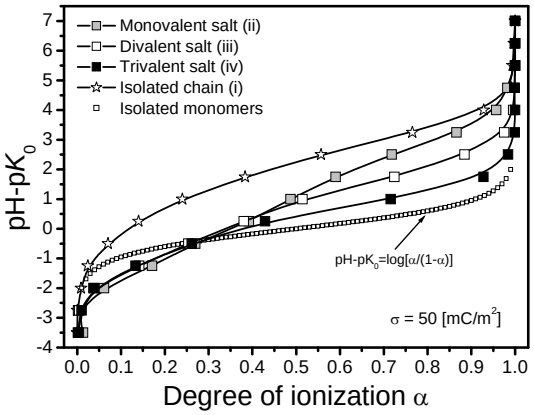

Fig. 2: Titration curves for (i) an isolated chain in presence of monovalent salt, as well as for a weak polyelectrolyte and one nanoparticle surrounded by (ii) monovalent, (iii) divalent and (iv) trivalent salt.

PBE breakage kernel through Stokesian Dynamics simulations of breakage of colloidal aggregates

Yogesh M. Harshe, Marco Lattuada, and Massimo Morbidelli

Institute for Chemical and Bioengineering, Department of Chemistry and Applied Biosciences, ETH Zurich, 8093 Zurich, Switzerland

Practically occurring processes of colloidal aggregates' production and their processing in sheared fluids involve the preparation of aggregates made of a large number of particles. Population balance equations (PBE), implementing aggregation and breakage kinetics, are commonly used to investigate and predict the evolution of aggregate formation under different conditions. However, PBE require lumped parameters, called kernels for both aggregation and breakage processes, to include all the physical information about the process. In the literature, the aggregation kernels are well established, whereas the breakage kernels hold a great degree of uncertainty as the aggregate breakup process is relatively more complex to study through experiments and/or to implement in aggregate motion models. We have formulated a model to study the breakup of colloidal aggregates made of identical spherical particles in shear flow under laminar flow conditions, using Stokesian dynamics to estimate the hydrodynamic interactions among the particles, DLVO theory to describe the normal inter-particle interactions, and discrete element method to account for the tangential contact interactions. Simulations were performed to study different characteristics of the breakage process of fractal aggregates, generated using different Monte-Carlo methods, composed of a number of uniform sized spheres and characterized by fractal dimensions, at different flow magnitudes in simple shear flow. The developed model was first used to investigate the dependence of the characteristic time required for the on-set of cluster breakage on the cluster geometry (mass and morphology) and flow conditions. In addition, the dependence of the fragment mass distribution at the instance of first breakage on the cluster mass and morphology has been studied. The so performed analysis of the breakage process was used to develop a breakage kernel which can be directly used in PBE.

Binding avidity and its Implications for transport through the nuclear pore complex

Larisa E. Kapinos, Rafael Schoch, Laura De Pasquale, Roderick Y. Lim

EPF Biozentrum and the Swiss Nanoscience Institute, University of Basel, Klingelbergstrasse 70, Basel 4056, Switzerland

Nuclear pore complexes (NPCs) regulate the selective exchange of macromolecular cargoes across the nuclear envelope. Access is limited to cargo-carrying transport receptors (e.g. importinß or impß), which interact with several Phe-Gly (FG) repeat rich domains (i.e. FG-domains) that are end-tethered in and around the NPC. The collective behavior of the FG-domains remains ambiguous. In particular, it is unclear how the FG-domains interact with the transport receptors to optimize NPC cargo translocation. It is known that: (i) each FG-domain is natively unfolded/intrinsically unstructured with multiple FG-repeat motifs, and (ii) each transport receptor has several FG-binding pockets. The purpose of this work is to understand (1) how FG-domain structure is dependent on surface density and (2) how this can affect receptor-FG binding interactions and consequently a transport through the nuclear pore. By Surface Plasmon Resonance (SPR) experiments we show that impß exhibits different binding affinities to different end-tethered FG-domains (Nup62, Nup98, Nup153 and Nup214). Importantly, the dissociation constant (KD) behaves non-monotonically as a function of the surface grafting density and suggests the existence of an optimal surface density, which maximizes the binding (avidity effect). Using a special approach in our SPR experiments and AFM measurements we correlate the binding affinity with the conformational changes of the FG-domain-layer upon impß binding. The most stable complex is proven to form when the receptor molecule can still penetrate the FG-domain-layer and interact with maximal number of FGs. As a result of such interaction a slight decrease of the layer thickness is observed (partial collapse). Further increase of the FG-domain surface density leads to the exclusion of importin ß from FG-domain-layer and decrease of binding affinity. Our results strongly indicate that the number and localization of each FG-domain in the NPC plays a key role in optimizing nucleocytoplasmic transport efficiency.

Melting and Crystallization Rates from MD Simulations

Konstantin Koschke[1], Davide Donadio[1], Hans-Jörg Limbach[2], Kurt Kremer[1]

[1] *Max-Planck Institute for Polymer Research, Mainz.* [2] *Nestlé Research Center, Lausanne*

Abstract

Molecular dynamics simulations extend the understanding of crystal growth and allow us to investigate the relevant processes on time and length scales that experiments cannot reach. In this work we plan to elucidate the basic atomistic mechanism of polymer-controlled crystallization and melting. In this initial phase we use the Lennard-Jones model system to set up a stable and reliable protocol to compute crystal growth and melting rates in non-equilibrium molecular dynamics of two-phase systems. Our results highlight the crucial effect of latent heat dissipation in decreasing crystallization and melting rates below the kinetic limit. To probe the kinetic growth limit we implement a modification of the stochastic rescaling thermostat, where the system is sliced into independent temperature coupling groups. We prove that this approach effectively removes latent heat locally, yielding a reliable estimate of the maximum crystallization/melting rate. This set-up is used to investigate the effect of additives on the crystallization process as a function of their size and concentration.

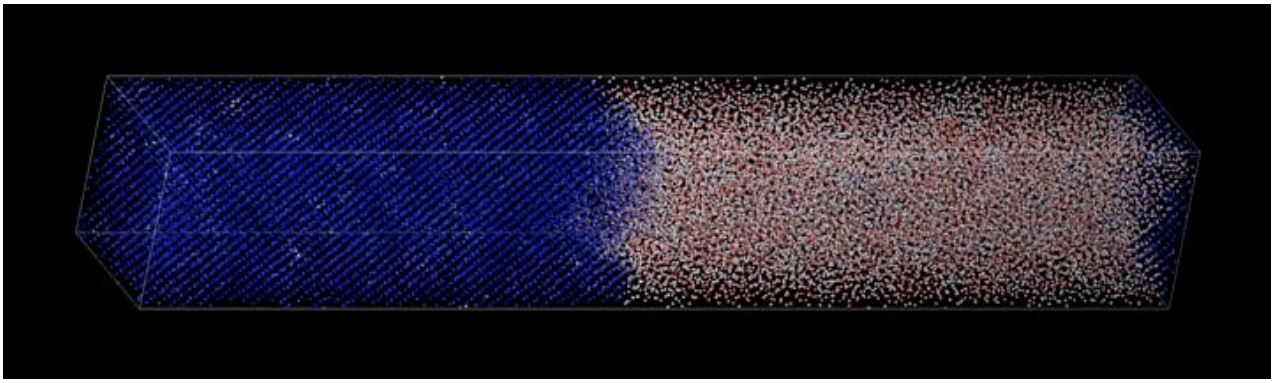

References:

[1] G. Fernández et al. J. Chem. Phys. 124:144506.

[2] D. van der Spoel et al. J. Comp. Chem. 26:1701-18.

[3] P. R. ten Wolde et al. J. Chem. Phys. 104:9932.

[4] V. Rühle et al. J. Chem. Theo. Comput. 5:3211-3223.

[5] G. Bussi et al. J. Chem. Phys 126:014101.

[6] J. Monk et al. Model. Simulat. Mater. Sci. Eng. 18:015004.

Flow of a long chain branched polymer melt in a cross-slot channel

M. Sadati*, C. Luap, M. Kröger and H. C. Öttinger
Department of Materials, Polymer Physics, ETH Zürich,
CH-8093 Zürich, Switzerland
**sadati@mat.ethz.ch*

A partially lubricated cross-slot channel rheometer producing strong extensional deformation in the stagnation region has been utilized to study the essentially two-dimensional complex flow behavior of a highly branched polyethylene melt. The kinematics of the complex flow was detected using particle tracking velocimetry. Subsequently, from these necessarily noisy experimental velocimetry data, the underlying full field kinematics was reconstructed by implementing a regularization based on the Tikhonov approach and a high order finite element approximation. In addition, the stress field was measured optically using flow induced birefringence (FIB). Results show that the presence of long chain branches in the polymer structure generates high stress values near the outflow centerline influencing both the flow kinematics and the birefringence pattern. A theoretical stress field was calculated by solving the established eXtended Pom-Pom (XPP) constitutive equation using the regularized experimental flow kinematics through integration over streamlines. Comparison between the XPP cross-slot predictions and experimental results elucidates that although the XPP model is able to provide overall good quantitative match, it fails to capture important details characteristic of the branched structure of the melt.

Effect of Quenched Size Polydispersity on the Fluid-Solid Transition in Charged Colloidal Suspensions

J.Colombo[1], M.Dijkstra[2]

[1] Institute for Building Materials, ETH Zürich, Zürich, Switzerland. [2] Soft Condensed Matter, Debye Institute for NanoMaterials Science, Utrecht University, Utrecht, The Netherlands.

We study the effect of quenched size polydispersity on the phase behavior of charged colloidal suspensions using free-energy calculations in Monte Carlo simulations. The colloids are assumed to interact with a hard-core repulsive Yukawa (screened-Coulomb) interaction with constant surface potential, so that the particles are polydisperse both in size and charge. In addition, we take the size distribution to be fixed in both the fluid and crystal phase (no size fractionation is allowed). We study the fluid–solid transition for various screening lengths and surface potentials, finding that upon increasing the size polydispersity the freezing transition shifts toward higher packing fractions and the density discontinuity between the two coexisting phases diminishes. Our results provide support for a terminal polydispersity above which the freezing transition disappears.

REFERENCE: J. Chem. Phys. **134**, 154504 (2011).

Synthesis and characterisation of hybrid α-Fe_2O_3/Fe_3O_4 anisotropic nanoparticles

I. Bobowska[1], S. Hengsberger[1], E. Vanoli[1], T. Chappuis[1], B. Grobéty[2], H. Dietsch[3]

[1] University of Applied Sciences, College of Engineering and Architecture of Fribourg, Fribourg, Switzerland. [2] Department of Geosciences, University of Fribourg, Fribourg, Switzerland.
[3] Adolphe Merkle Institute, University of Fribourg, Fribourg, Switzerland.

INTRODUCTION: α-Fe_2O_3 (hematite) and Fe_3O_4 (magnetite) nanoparticles are interesting objects for interaction studies of magnetic colloids. Hematite nanoparticles only exhibit weak ferromagnetic properties [1]; however they can be easily synthesized in the form of anisotropic spindle shaped nanoparticles by wet chemistry methods [2]. Magnetite nanoparticles show a very strong magnetic response because of their highly ferrimagnetic or even superparamagnetic (for crystals smaller than 15 nm) properties [1]. Tailored magnetic response can be achieved by partial transformation of the easily synthesized hematite nanoparticles into magnetite. The goal of this work is to perform a controlled transformation process of hematite spindle-type nanoparticles in autoclave conditions, under hydrogen gas pressure, with fixing anisotropic particles morphology and tuning crystalline structure.

METHODS*:* Spindle-type hematite (α-Fe_2O_3) particles, are synthesized by the forced hydrolysis of $Fe(ClO_4)_3$, according to Ocaña et al. [2]. The upscaled synthesis is made in 15 liter Hastelloy reactor. A 693.6g of $Fe(ClO_4)_3 \cdot 6H_2O$, 90.07g of urea and 9.73g of NaH_2PO_4 dissolved in 15 liters of MilliQ water is heated (100°C, 24h). A precipitate is collected by centrifuging, washing with MilliQ water and drying (24h, 98°C). The reduction process is performed in a customer-made 10ml autoclave installation connected with a hydrogen (H_2) bottle (for reduction) or a nitrogen (N_2) bottle (for flushing). A 0.2g of hematite is annealed at 300°C in a H_2 atmosphere under a constant pressure (11 bars). Temperature and pressure are maintained for 8 to 45 hours of H_2 treatment. Transmission Electron Microscope (TEM-CM100, Philips) operating at 80 kV is used for size and morphology characterisation. Powder X-ray diffraction (XRD) patterns of the samples are measured with a (Philips, PW1800) diffractometer (Cu-tube). The XRD spectra are fitted employing hematite and magnetite crystalline structures using the Rietveld method and the TOPAS3 software package (Bruker Inc.)

RESULTS: Spindle type morphology of hematite nanoparticles with a long axis of 284 ± 45 nm and a short axis of 51,8 ± 7,1 nm is illustrated on Fig.1a.
Fig.1b and Fig.1c show particles obtained after 10 and 20 hours of hydrogen treatment.

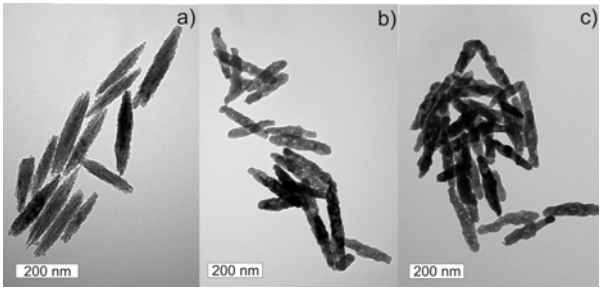

Fig. 1: TEM images for hematite nanoparticles after: a) – 0h, b) – 10h, c) – 20h of H_2 treatment.

As a result of the heat treatment the surface of the nanoparticles becomes more porous, the anisotropy of the shape is preserved and about 10 - 20% reduction of dimensions is observed. XRD analysis combined with Rietveld refinement show an increase of magnetite phase content in the reduced samples with prolongation of H_2 treatment. A 45h of H_2 treatment gives 94wt.% of magnetite content.

DISCUSSION & CONCLUSIONS: As a result of H_2 treatment the spindle-type morphology of nanoparticles is only slightly affected. A weak shrinkage is observed that is probably caused by the crystalline transformation from hematite to magnetite, what is confirmed by XRD. This study showed that the stoechiometry of hematite and magnetite content in the reduced nanoparticles can be tailored by controlling the time of H_2 treatment.

REFERENCES: [1] R.M. Cornell, *The Iron Oxides: Structures, Properties, Reactions, Occurrences and Uses,* Wiley-VCH, Weinheim, **2003**.
[2] M. Ocaña; **1999**; *J. Colloid Interface Sci.*; 212: 317-323.

ACKNOWLEDGEMENTS: This work is supported by the Sciex-NMS^{ch} (Project Code 10.007), and the Adolphe Merkle Foundation.

Nanostructures using amphiphilic peptides

T. Schuster, D. de Bruyn, W. Meier

University of Basel, Klingelbergstrasse 80, 4056 Basel, Switzerland

INTRODUCTION: Nanostructures that range from micelles and vesicles to fibres and solid spheres lend themselves to a wide variety of applications. These include the design of specifically structured surfaces, e.g. those of implants. In terms of materials, limitations arise when used in the human body. Biomaterials such as peptides can be designed to fulfil desired morphologies and properties. Because they are based on amino acids, they can be eliminated through intrinsic bodily degradation pathways.

METHODS: Fmoc-based solid-phase peptide synthesis on Rink Amide AM was used, with HCTU/DIPEA as the coupling reagent. Double RP-HPLC with acetonitrile/aq. buffer gradients (0.1% TFA and 2% AcOH) yielded material with purities ≥ 95%. Self-assembly was induced by dissolving the peptide in ethanol, followed by dialysis against water. Transmission and scanning electron microscopy (TEM, SEM), dynamic and static light scattering (DLS, SLS) as well as small angle X-ray scattering (SAXS) were used for characterisation.

RESULTS: Various purely amphiphilic peptides have been develop to self-assemble into a diversity of nanostructures that range from micelles and fibers to vesicles and solid nanospheres[1]. As they provide hydrophobic regions, micelles tend to host materials such as water insoluble dyes in their cores. Due to the structure of their membranes, vesicles also exhibit this property but additionally encapsulate hydrophilic substances in their aqueous cavities. Thus, vesicles possess the ability to co-encapsulate, making them a preferred morphology. However, loading efficiencies may be low, due to the process by which they are formed, while the volumes of hydrophilic and hydrophobic compartments are not equal. Multicompartment micelles (MCM) offer balanced volumes to accommodate different substances. Amphiphilic peptides Ac-X_3-gT assemble into spherical nanospheres, referred to as peptide beads which are thought to exhibit MCM structure. This was indicated by the encapsulation of gold nanoparticles (Au-NP) in micellar cores of AcC-X3-gT, which was followed by the induction of peptide bead formation (*Figure 1*). Final proof was demonstrated by SAXS measurement, confirming a MCM structure.

Table 1. Code and sequence of charged (K) and uncharged (X = LK(Ac)) amphiphilic peptides.

Code	Sequence
Ac-X_3-gT	*Ac*-LX$_3$-[LW-DL]$_3$-LW-*NH$_2$*
AcC-X_3-gT	*Ac*-LC-LX$_3$-[LW-DL]$_3$-LW-*NH$_2$*

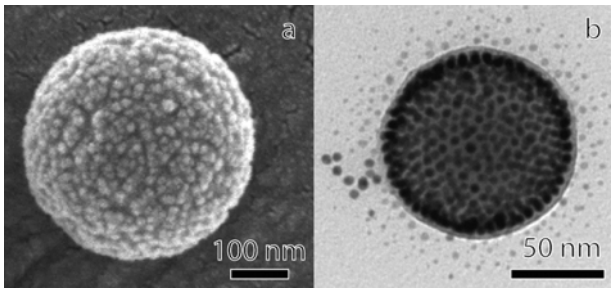

Fig. 1:a) SEM and b) TEM of Au-NP peptide beads

DISCUSSION & CONCLUSIONS: The underlying morphology of our peptidic nanoparticles was elucidated on the basis of structural investigations. Previous experiments on the encapsulation of different dyes of high loading efficiencies are thereby explained. The results further open the door for rational encapsulation and embedding and may be of interest in developing a multitude of applications.

REFERENCES: [1] de Bruyn Ouboter, D.; Schuster, T.; Mantion, A.; Meier, W. 2011, submitted

ACKNOWLEDGEMENTS: Financial support by the SNSF and the NCCR Nanosciences is gratefully acknowledged. The authors thank the ZMB, Prof. H. Wennemers, Dr. A. Mantion, and M. Inglin.

Controlling membrane permeability with channel proteins

Ozana Onaca-Fischer

University of Basel, Basel, Switzerland, ozana.onaca@unibas.ch.

Recently block copolymer vesicles (polymersomes) have been introduced as promising candidates for drug delivery applications. Polymersomes are mechanically and chemically more stable than their biological counterparts – liposomes [1]. However the permeability of the polymeric membranes is lower than the one of liposomes. Channel proteins (OmpF, FhuA, AqpZ, LamB, Tsx) have been used to increase and control the permeability of polymeric membranes [2].

We present here two channel proteins (OmpF and FhuA) that have been genetically engineered to control the transport of molecules across polymeric membranes.

FhuA (Ferric hydroxamate component A) has been designed as a passive diffusion channel by removal of the globular domain present inside the wild type. The modified channel has been further functionalized with ligands of various sizes containing disulphide bridges. Upon breakage of the disulphide bonds, the channel proteins are unblocked and allow in a controlled manner passive transport of molecules across them (Fig 1) [3].

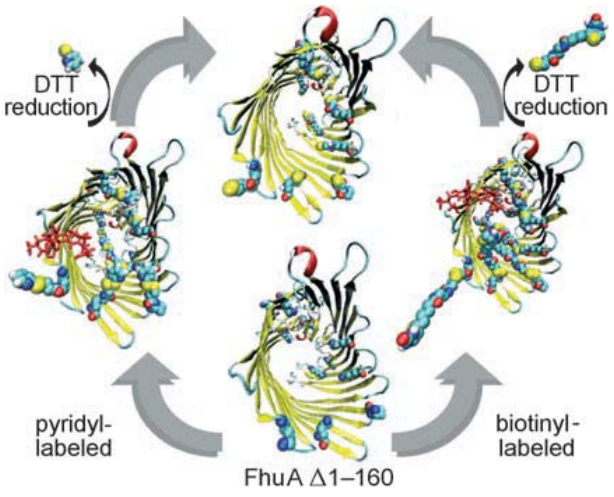

Fig. 1: Reduction-triggered release system based on transmembrane channel FhuA D1–160. FhuA D1–160 is chemically modified with pyridyl or biotinyl labels at lysine residues in the barrel interior and at the rim.

OmpF (Outer membrane protein F) has been genetically modified by substituting six amino-acids with histidines inside the barrel (Fig 2). [3]

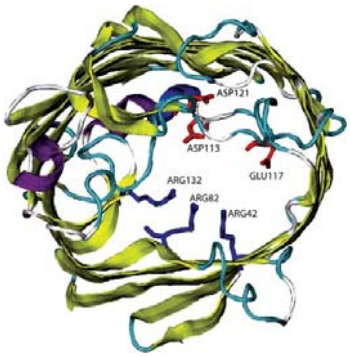

Fig. 2: *Monomer of OmpF transmembrane channel (top view) with constriction region and highlighted two half-rings (Arg42, Arg82, Arg132, Asp113, Glu117 and Asp121).*

The six histidines have formed a ring inside the barrel that has responded electrostatically and geometrically to the external changes of pH [4].

The reduction-triggered release system and the pH switchable channel proteins have been tested in polymeric vesicles made of PMOXA-PDMS-PMOXA block copolymers. Polymersomes reconstituting responsive channels proteins have great potential especially in controlled drug delivery. Taking advantage of the possibility of specifically targeting polymersomes, the resulting functionalized responsive polymer vesicle assembly can be of special interest in therapeutic and diagnostic applications.

REFERENCES:

1.Discher, B.M., Won, Y.Y., Ege, D.S., Lee, J.C.M., Bates, F.S., Discher,D.E., Hammer, D.A., 1999. Science 284, 1143.

2. P. Baumann, P. Tanner, O. Onaca, C. Palivan, 2011. Polymers, 3, 172.

3. O. Onaca, P. Sarkar, D. Roccatano, T. Friedrich, B. Hauer, M. Grzelakowski, A. Guven, M. Fioroni, U. Schwaneberg, Angew. Chem., Int. Ed., 2008. 47, 7029.

4. S. Ihle, O. Onaca, P. Riegler, B. Hauer, F. R. Ropero, M. Fioroni, U. Schwaneberg, Soft Matter, 2011. 7, 532.

ACKNOWLEDGEMENTS: Financial support was provided by the Swiss National Science Foundation.

Up-converting nano-phosphors for bioimaging and bio-oxidations

M. Crittin[1], M. Schaer[2], A. Fink[3], L. Forró[1], and A. Sienkiewicz[1]
[1]*Institute of Condensed Matter Physics, School of Basic Sciences, EPFL, Lausanne, Switzerland*
[2]*Institute of Materials, School of Engineering, EPFL, Lausanne, Switzerland*
[3]*Advanced Particle Group, University of Fribourg, Switzerland*

INTRODUCTION: Near-infrared (NIR) fluorescence is gaining increasing attention as analytical tool in imaging *in vitro* and *in vivo* [1]. The NIR region is also attractive for several medical applications, where the deep penetration of light into tissues is of utmost importance. Photo-luminescent NIR-to-visible-light up-converting $NaYF_4:Yb^{3+},Er^{3+}$ nanocrystals are ideally suited for *in vivo* photo-luminescence bio-imaging and performing deep-tissue photo-chemical reactions, including cancer tissue eradication in photodynamic therapy (PDT) *via* selective photo-oxidation of diseased tissues [2,3]. The commercially available $NaYF_4:Yb^{3+},Er^{3+}$ powders have good photo-optical properties but their typical grain sizes are usually too big for biological applications, which require sub-50 nm sizes. On the other hand, the custom fabrication of nano-sized up-converting phosphors having satisfactory photo-optical properties for biomedical applications remains still a big challenge [4]. Here, we report preparation of highly photo-efficient powdered phosphors by mechanical grinding of the commercially available $NaYF_4:Yb^{3+},Er^{3+}$. We measured both the phosphorescence efficacy of the ground powders and their potential towards performing local bio-oxidative processes. The ground material was also used to perform preliminary imaging experiments in worms, *C.elegans*.

METHODS: The commercial $NaYF_4:Yb^{3+},Er^{3+}$ up-converting material, PTIR550/F, from Phosphor Technology, Ltd. (England) was ground using ZrO_2 grinding balls (diameter 1.25 mm) for 2 hours at rotation speed of 1500 rpm. The obtained particles were characterized with transmission electron microscopy (TEM), X-ray diffraction (XRD) and dynamic light scattering (DLS). Thin PMMA films loaded with the ground materials were prepared by spin-coating on glass substrates and the phosphorescence spectra were acquired under excitation with 980 nm NIR light using a custom-made spectro-fluorometer designed around a commercial diode-array-based spectrometer from Ocean Optics, Model QE-65000. NIR-light-induced formation of reactive oxygen species (ROS) was performed with reactive scavenging followed by electron spin resonance (ESR) detection.

RESULTS: The TEM images and DLS characterization provided evidence that the ball-milling reduced the median particle sizes from *ca.* ~ 4.1 μm to 0.4 μm. The XRD patterns obtained for the ground confirmed the presence of the highly-phosphorescent hexagonal crystalline phase.

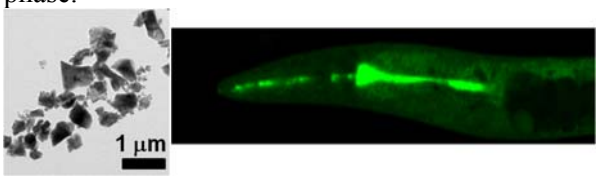

Fig. 1: TEM image of the ground material (left) and the confocal microscopy image obtained under NIR-light illumination for C.elegans fed on the ground up-converting phosphor (right).

DISCUSSION & CONCLUSIONS: The one-step ball-milling process of the commercial up-converting phosphors yielded ~ 10 times smaller particles, having mean particle sizes in the range of hundreds of nanometers. The milled particles revealed satisfactory photo-optical properties for bioimaging and performing local bio-oxidations *via* NIR light-induced generation of ROS.

REFERENCES: [1]S.F. Lim, R. Riehn, C.-K. Tung, W.S. Ryu, R. Zhuo, J. Dalland, and R.H. Austin; **2009**; *Nanotechnology*; 20: 405701-6. [2]K.W. Krämer, D. Biner, G. Frei, H.U. Güdel, M.P. Hehlen, and S.R. Lüthi; **2004**; *Chemistry of Materials*; 16: 1244-1251. [3]H.S. Mader, P. Kele, S.M. Saleh, and O.S. Wolfbeis; **2010**; *Current Opinion in Chemical Biology*; 14: 582-596. [4]C. Liu, H. Wang, X. Li, and D. Chen; **2009**; *J. Mater. Chem.*; 19: 3546-3553.

ACKNOWLEDGEMENTS: We acknowledge the financial support of the Swiss Nano-Tera NTF project "NanoUp". We also thank Prof. Pierre Gönczy and Coralie Busso (both from the EPFL) for providing worms *C.elegans* for this study.

Nanocluster preparation through aggregation and breakage processes

FABIO CODARI, MIROSLAV SOOS , DAVIDE MOSCATELLI[1], MASSIMO MORBIDELLI

Institute for Chemical and Bioengineering, Department of Chemistry and Applied Biosciences, ETH Zurich, Wolfgang Pauli strasse 10, CH-8093 Zurich (Switzerland)

[1] Dipartimento di Chimica, Materiali e Ingegneria Chimica ''Giulio Natta'', Politecnico di Milano, Milano, Italy

miroslav.soos@chem.ethz.ch

Abstract

Nanoclusters (NCs) obtained by aggregation of primary nanoparticles (NPs) find application in different research and industrial fields ranging from food and cosmetic to pharmaceutical products. Even if they present large interest, current understanding of the physical processes involved (i.e. aggregation, breakup and restructuring) in their production is still lacking. NPs size and chemical composition together with NCs structure and size are fundamental aspects which affect the final product features and application. The aim of the present work is to investigate the production of NCs on the base of selected key parameters, such as NPs size, surface charge type, charge density, stabilizer nature and system fluid dynamics.

In a first step, polymeric primary NPs of PMMA and PLA with different surface charge density and with particle size ranging from 15 to 200 nm, were produced through starved emulsion polymerization and flash nanoprecipitation in multi inlet vortex mixer (MIVM). To better understand the mechanism of polymer particle formation and the effect of operating parameters on final particle size a systematic study on the effect of selected parameters such as polymer molecular weight and concentration, role of surfactant and geometry of the mixer was carried out. Moreover, NP of silica and magnetite were used as prototype for inorganic materials. After production, the NPs were aggregated in DLCA regime producing large clusters of several microns in diameter by addition of an electrolyte solution. Surfactant was then added to the cluster dispersion and controlled breakage was used to reduce size of clusters down to submicron scale. To obtain well define conditions during breakage, characterized by CFD, suspension was pumped through contracting nozzle. Characterization of NCs size and structure was carried out by light scattering analysis and TEM. Different surfactants, such as Tween 80, PVA and CTAB, and different concentrations, ranging from 0.5 to 50 surfactant polymer ratio, were investigated. Results show a clear dependence of NCs size upon the selected operating conditions. In particular for polymeric NP, the final cluster size is independent upon the nature of surfactant used and primary particles size while a strong role is played by the nature of the primary particle material and shear rate. The experimental findings are used to construct a reliable tool for tailor made production of NCs for specific applications.

A new tool for controlled siRNA delivery: polymer-protein core-shell hybrid

M. G. Nussbaumer[1], N. Bruns[2]

[1] *University of Basel, Basel, Switzerland.*

INTRODUCTION: Polymer nanoparticles and drug-polymer conjugates are highly important in modern drug delivery technology, as they can be tailored to fulfill several functions [1]. Polymers, particularly highly branched or dendrimeric polymers, are considered to be used as drug delivery vehicles. The advantages of such polymers are that they can bind or incorporate drugs, whereas their surface can be functionalized with targeting and/or reporting agents. Furthermore, the polymers can be designed to release their payload depending on the environmental conditions such as pH or temperature. Cationic polymers such as polyamidoamine (PAMAM) are able to form a complex with RNA or DNA [2]. A drawback of these cationic polymers is their toxicity to cells due to their positively charged surface. Several attempts to overcome this problem are based on the modification of their surface. But this reduces the ability of binding nucleic acids. Therefore, we incorporated PAMAM into the protein cage thermosome, a chaperonin from *Thermoplasma acidophilum*. The thermosome provides a closable cavity large enough to accommodate macromolecules such as PAMAM. Our concept is that PAMAM in the thermosome can bind small interfering RNA (siRNA), thus acting as an anchor to entrap oligonucleotides. The protein shell around a PAMAM-siRNA complex would protect encapsulated oligonucleotides against degradation and shields the positive charges of the polymer from the cells.

METHODS: A bisarylhydrzone linker was used to obtain the polymer-protein core-shell hybrid using thermosome and PAMAM (generation 4). To this end, PAMAM was functionalized with a succinimidyl functionalized 6-hydrazinonicotinamide (S-HyNic) which reacts with primary amines of the PAMAM surface via succinimidyl chemistry. Thermosome was functionalized with maleimido trioxa-6-formyl benzamide (MTFB). An engineered thermosome was used that only possess accessible cysteins at the interior surface of the thermosome β-subunit [6], so that the MTFB attaches to the inner wall of the cavities. The purification of modified PAMAM and THS from excess linkers was carried out by extensive ultra-filtration. The aromatic hydrazine on the PAMAM surface and the aromatic aldehyde at the interior of the thermosome react under mild conditions to form a resonance stabilized Schiff's base. The conjugation reaction was done at pH 6.5 overnight at room temperature. Size exclusion chromatography was used to separate the polymer-protein core-shell hybrid from free PAMAM. Free PAMAM and the thermosome-PAMAM complex were baseline-separated.

RESULTS: To verify the conjugation, UV-spectroscopy was carried out, among others. The formed bisarylhydrazone linker absorbs UV light at a specific wavelength (λ = 354 nm). The UV-Vis spectrum in Figure 1 reveals an overlay of two main peaks: A peak at around 280 nm from the thermosome and a peak at 354 nm originating from the newly formed bisarylhydrazone bond. From this spectrum the ratio of PAMAM per thermosome was calculated to about three.

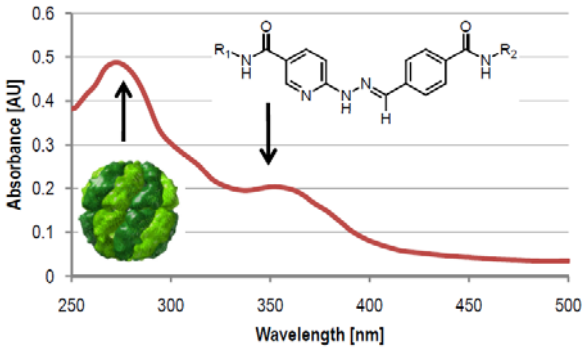

Fig. 1: UV-Vis-absorbance spectrum of thermosome-PAMAM conjugate.

DISCUSSION & CONCLUSIONS: We conclude a successful linking of PAMAM into the thermosome. The linking chemistry does not harm the protein and is therefore suitable for linking of polymer to protein. This polymer-protein core-shell hybrid should be able to take up drug payload and to hide the PAMAM so that, the cationic surface of PAMAM, which is needed to complex siRNA, is shielded from the cells.

REFERENCES: [1] Kim, S.; **2009**; *Eur. J. Pharm. Biopharm*; 71, 420.

[2] Zhou, J; **2006**; *Chem. Comm.*; 2362

Aggregation stability of therapeutic proteins in downstream processing

Paolo Arosio, Simonetta Rima, Baptiste Jacquet, Hua Wu and Massimo Morbidelli

Institute for Chemical and Bioengineering, Department of Chemistry and Applied Biosciences, ETH Zurich, 8093 Zurich, Switzerland.

paolo.arosio@chem.ethz.ch, Fax: +41 44 6321082

Therapeutic proteins represent a fast growing class of drugs in the pharmaceutical market. Achieving a better understanding of the mechanisms responsible for protein aggregation is crucial for successful commercialization of protein drugs. In this work, we investigate the aggregation stability of several monoclonal antibodies (mAbs) in conditions relevant for downstream processing. The time evolution of the aggregates is analyzed by a combination of dynamic light scattering, size exclusion chromatography and field flow fractionation. Secondary structure changes are monitored by circular dichroism and thioflavin binding.

The results get insights into the intricate combined effect of pH, salt concentration, nature of salt, temperature and antibody class on aggregation stability. Depending on operating conditions either reversible oligomerization or aggregation into insoluble, high molecular weight aggregates may occur. The experimental results are rationalized by providing a mechanistic description of both processes which connects the aggregation kinetics to the protein conformational stability and colloidal stability.

Particularly, an anion specific effect in inducing aggregation is observed according to a ranking which follows the Hofmeister series with the exception of the sulfate anion.

References:

P. Arosio, G. Barolo, T. Müller-Späth, H. Wu, and M. Morbidelli, *Pharmaceutical Research*; **2011**, *in press*

Contact list of participants

First Name	Name	E-Mail
Christof	Aegerter	aegerter@physik.uzh.ch
Paolo	Arosio	paolo.arosio@chem.ethz.ch
Vimalkumar	Balasubramanian	v.balasubramanian@unibas.ch
Patric	Baumann	patric.baumann@unibas.ch
Maxim	Belushkin	maxim.belushkin@epfl.ch
Fabrizio	Benedetti	fabrizio.benedetti@epfl.ch
Elena	Bertseva	elena.bertseva@epfl.ch
Irmgard	Bischofberger	irmgard.bischofberger@unifr.ch
Noemi	Blanchard	noemi.blanchard@unifr.ch
Izabela	Bobowska	izabela.bobowska@hefr.ch
Arturo	Bohm	arturo.bohm@buhlergroup.com
marco	Braibanti	marco.braibanti@unifr.ch
Nico	Bruns	nico.bruns@unibas.ch
Saskia	Bucciarelli	saskia.bucciarelli@unifr.ch
Etienne	Cabane	etienne.cabane@unibas.ch
Fabrice	Carnal	fabrice.carnal@unige.ch
Jader	Colombo	jader@ifb.baug.ethz.ch
Dirk	de Bruyn	dirk.debruyn@unibas.ch
Emanuela	Del Gado	delgadoe@ethz.ch
Mihaela	Delcea	mihaela.delcea@unibas.ch
Siddharth	Deshpande	s.deshpande@unibas.ch
Herve	Dietsch	herve.dietsch@unifr.ch
Dominik	Dobrunz	dominik.dobrun@unibas.ch
Zhaofu	Fei	zhaofu.fei@epfl.ch
Davide	Fiocco	davide.fiocco@epfl.ch
Andreas	Fisch	andreas.fisch@novartis.com
Peter	Fischer	peter.fischer@ilw.agrl.ethz.ch
Ozana	Fischer	ozana.onaca@unibas.ch
Giuseppe	Foffi	giuseppe.foffi@epfl.ch
Urs	Gasser	urs.gasser@psi.ch
Juan Carlos	Germain	juancarlos.germainguzman@rdls.nestle.com
Deniz	Gunes	zeyneldeniz.gunes@rdls.nestle.com
Jakub	Haberko	jakub.haberko@unifr.ch
Yogesh	Harshe	yogesh.harshe@chem.ethz.ch
Axel	Hochstetter	axel.hochstetter@unibas.ch
Joerg	Huwyler	Joerg.Huwyler@unibas.ch
Katerina	Ioannidou	katerinaioannidou@ethz.ch
Lucio	Isa	lucio.isa@mat.ethz.ch
Fabian	Itel	fabian.itel@unibas.ch
Agnieszka	Jagoda	agnieszka.jagoda@unibas.ch

Mehdi	Jorfi	mehdi.jorfi@unifr.ch
Corinne	Jud	corinne.jud@unifr.ch
Larisa	Kapinos	larisa.kapinos@unibas.ch
Dawid	Kedracki	dawid.kedracki@unige.ch
Marzena	Kocik	m.kocik@unibas.ch
Justyna	Kowal	justyna.kowal@unibas.ch
Karolina	Langowska	karolina.langowska@unibas.ch
Cecile	Lara	celara@ethz.ch
Marco	Lattuada	marco.lattuada@chem.ethz.ch
Hans Joerg	Limbach	hans-joerg.limbach@rdls.nestle.com
Carlo	Maffi	carlo.maffi@epfl.ch
Raffaello	Masciadri	raffaello.masciadri@bluewin.ch
Hossein	Naseri	Hossein.Naseri@unifr.ch
Renata	Negrini	rnegrini@ethz.ch
Biagio	Nigro	biagio.nigro@epfl.ch
Martin	Nussbaumer	martin.nussbaumer@unibas.ch
Ivan	Orlov	ivan.orlov@epfl.ch
Cornelia G.	Palivan	Cornelia.Palivan@unibas.ch
Philippe	Polleux	philippe.polleux@unibas.ch
Johannes	Reinhardt	Johannes.Reinhardt@unifr.ch
Kasper	Renggli	Kasper.Renggli@unibas.ch
Walter	Richtering	richtering@rwth-aachen.de
Daniel	Ross	daniel.ross@unifr.ch
Monirosadat	Sadati	sadati@mat.ethz.ch
Giuseppe	Scalia	giuseppe.scalia@unifr.ch
Thomas	Schuster	thomas.schuster@unibas.ch
Andrzej	Sienkiewicz	andrzej.sienkiewicz@epfl.ch
Reinhard	Sigel	reinhard.sigel@unifr.ch
Tilana	Silva	tilana.silva@gmail.com
Umut	Soydaner	umut.soydaner@stud.unibas.ch
Adriana Cristina	Toma	adriana.toma@unibas.ch
Smahan	Toughrai	smahan.toughrai@unibas.ch
Veronique	Trappe	Veronique.Trappe@unifr.ch
Kitty	van Gruijthuijsen	kitty.vangruijthuijsen@unifr.ch
Corinne	Vebert	corinne.vebert@unige.ch
Cedric Xing Ye	Yon	thiscedric87@gmail.com
Alexandru	Zabara	alexandru.zabara@agrl.ethz.ch
Xiaoyan	Zhang	xiaoyan.zhang@unibas.ch
Rakiya	Miluseva	rumilusheva@gmail.com